BOR DERGİSİ
JOURNAL OF BORON
https://dergipark.org.tr/boron

Development of PCL/PVA/PCL scaffold for local delivery of calcium fructoborate for bone tissue engineering

Ali Deniz Dalgic [1,*]

[1]*İstanbul Bilgi University, Faculty of Engineering and Natural Sciences, Department of Genetics and Bioengineering, İstanbul, 34060, Türkiye*

ARTICLE INFO

Article history:
Received September 13, 2024
Accepted October 14, 2024
Available online December 31, 2024

Research Article

DOI: 10.30728/boron.1549809

Keywords:
Bone tissue engineering
Boron
Calcium fructoborate
Polycaprolactone
Polyvinyl alcohol

ABSTRACT

Calcium fructoborate (CaFB) has gathered attention due to its boron and calcium content, both of which are known to support bone health, deposition and regeneration. Previous studies have shown that CaFB has a positive effect on bone health and has been proven to promote bone-like properties. In light of this information, a local CaFB delivering scaffold could improve bone regeneration in cases of bone tissue loss. This study aimed to design a layer-by-layer polymeric sponge capable of achieving controlled local delivery of CaFB to improve bone tissue healing. The dose-dependent effect of CaFB on the cell viability of the Saos-2 cell line was investigated *in vitro*. Layer-by-layer structure of the polymeric scaffold supported controlled release of CaFB, with 33.9±7.4% released after 7 days of incubation. CaFB at 31.25 µg/mL concentration was able to improve Saos-2 cell viability up to 174.7±24.1% and 127.7±8.7% after 1 and 4 days of incubation. After 7 days of incubation CaFB treatment at concentrations of 250, 125, 62.5 and 31.25 µg/mL improved cell viability up to 194.3±47.7, 155.3±17.7, 149.4±5.4 and 132.5±13.3%. The polycaprolactone/polyvinyl alcohol/polycaprolactone (PCL/PVA/PCL) scaffold supported the viability of cells for 7 days and was shown to be biocompatible. The results of this study showed that CaFB is a potential compound that can be locally delivered within a scaffold system to improve bone tissue regeneration.

1. Introduction

Boron is a trace element that exhibits both metal and non-metal properties and has several beneficial effects on human health such as influencing calcium metabolism, enhancing bone growth, and affecting nutrient and hormone metabolism. The main source of boron for humans is diet. Only plants can directly metabolize boric acid and borate compounds, converting them into monoester or diester forms, which are then consumed by humans and animals. Boron is essential for enhancing bone growth and strength. Boron is also known for its ability to regulate vitamin D metabolism, which has been shown to positively affect bone growth and differentiation [1,2]. Also, increased boron supplementation has been attributed to improved serum levels of vitamin D in deficient subjects [3]. Previous *in vitro* and *in vivo* studies have reported that boron can improve bone regeneration and strength [4-9]. When interacted with osteoblast cells, even at low doses, boron has been reported to activate cell proliferation and differentiation [10]. Similarly, low doses of boron have been shown to promote the expression of osteogenic markers, like collagen type I, osteopontin, bone sialoprotein, osteocalcin and runX2 while increasing levels of bone morphogenetic proteins (BMP-4, -6, -7) [9]. *In vivo* studies have shown a strong relation between increased bone strength and boron supplementation in Weanling pigs [5] and Sprague Dawley rats [6]. The positive effects of boron containing biomaterials on bone tissue healing are well defined in the literature. Boron bearing materials like bone cement, boron-doped hydroxyapatite (HAp), bioactive glasses, nanofibers and 3D-printed polymeric matrixes have been fabricated and shown to improve structural properties as well as bioactivity for bone regeneration [11-13].

Fructoborates are organic compounds consisting of boron and fructose and are naturally found in several fruits like apples, pears, and grapes [1]. Fructoborates exhibit no toxicity and accumulation and show better absorption than other boron compounds. Among fructoborates, calcium fructoborate (CaFB) has drawn attention for human health due to its calcium content [14]. CaFB can also be synthetically produced by allowing boric acid to form complexes with organic compounds like d-fructose [15]. Calcium, the other key component of CaFB, is a well-known ion that has been proven to support bone growth and strength by benefiting bone metabolism [16-18]. *In vivo* studies with CaFB have shown that CaFB can be systemically absorbed by the body [14,19]. When CaFB is taken via

*Corresponding author: deniz.dalgic@bilgi.edu.tr

diet, low pH in the stomach and enzymes can catalyze the hydrolysis of ester bonds to form fructose and boric acid which can be readily absorbed [20].

CaFB supplementation has been reported to stimulate osteoblast for mineralization when introduced along with dexamethasone [21]. In a pilot study, CaFB, when supplemented for six months, was reported to improve bone density in subjects with osteoporosis [22]. CaFB has also been incorporated into the surface coating of hydroxyapatite-coated titanium samples where its rapid release was reported to promote osteointegration [23]. CaFB can also improve bone health by regulating vitamin D metabolism. A previous pilot clinical trial has shown that boron supplementation in the form of CaFB can increase serum vitamin D and can be effective in improving bone and joint health in elderly patients [3]. Inflammation is another factor that is associated with bone loss due to increased osteoclastogenesis by proinflammatory cytokines and bone resorption. CaFB has been shown to lower inflammation by interacting with inflammatory molecules at cellular and enzymatic level, modulating the serum levels of reactive protein C (CRP) and other cytokines [19,24]. Today, as an alternative boron source, CaFB supplement products are available. Study by Marone et al. has evaluated the safety of CaFB supplements with an *in vivo* study and demonstrated that CaFB products have no mutagenic or genotoxic potential while no adverse toxicologic effects were found after a 90-day sub-chronic toxicology study [25].

These findings support the idea that a controlled local delivery system for CaFB could improve bone tissue regeneration by enhancing osteogenesis and osteoconduction. CaFB is a water-soluble molecule, that is why CaFB release from a traditional hydrogel is expected to be fast by water diffusion. If a CaFB-loaded hydrogel is implanted into the body, CaFB could be lost in a very short period and cannot sustain a therapeutic dose over bone tissue healing time. This reveals the need for a novel biodegradable scaffold that can control the local release of CaFB and sustain steady release over healing time. In light of previous literature, this study hypothesizes that local CaFB delivery can improve bone tissue regeneration, and a biodegradable polymeric scaffold can sustain a controlled release of CaFB. To achieve controlled release of CaFB, this study aimed to design a layer-by-layer polymeric scaffold (PCL/PVA/PCL) as a local delivery system. CaFB-loaded PCL/PVA/PCL scaffold was prepared from poly(ε-caprolactone) (PCL) and polyvinyl alcohol (PVA) polymers using consecutive freeze-drying steps.

Layer-by-layer scaffold fabrication for PCL and PVA has previously been reported for technologies like 3D printing and electrospinning [26,27]. The layered formation has enabled composites of polymers with different chemistry to be fabricated into the same scaffold which allows to tailor drug release and degradation rate [26]. PVA is a hydrophilic polymer that can be degraded in a short time in the body which causes the loss of mechanical strength. To support the mechanical strength of the scaffold, a synthetic polymer like PCL that has slower biodegradation should be used to form a composite [28,29]. In this study, freeze-drying technique was used to produce PCL/PVA/PCL composite scaffold which will carry CaFB in the core PVA layer. PCL layer was formed around the PVA to control the release rate and support the tissue mechanically through healing.

The fabricated scaffold was analyzed in terms of micro- and nano-morphology, time-dependent weight loss, and the capacity of PCL/PVA/PCL scaffold to controlling the release of CaFB. *In vitro* cell viability studies were conducted using Saos-2 (Human osteosarcoma cell line) cells which exhibit an osteoblast phenotype and have shown to be successful in replicating primary human osteoblast interaction with biomaterials [30]. Initially, the effect of CaFB on bone cells was analyzed in detail using i*n vitro* cell culture techniques to assess Saos-2 cell viability under varying concentrations of CaFB. Then, the effect of CaFB-loaded PCL/PVA/PCL scaffold was analyzed via direct incubation of cells on the scaffold surface via an *in vitro* cell viability test.

2. Materials and Methods

2.1. Fabrication of Layer-by-Layer Scaffold

The tri-layered scaffold was fabricated using PCL (Mw: 70.000-90.000 g/mol, Sigma-Aldrich, USA) and PVA (Mw: 72.000 g/mol, Sigma-Aldrich, USA) polymers. Compositions of experimental groups are presented in Table 1 and the steps of scaffold fabrication are presented in Figure 1a.

Table 1. Percent weight composition of experimental groups PVA and PCL/PVA/PCL

Sample ID	Materials					
	PVA		PCL		CaFB	
	wt (mg)	wt (%)	wt (mg)	wt (%)	wt (mg)	wt (%)
PVA	50	95.2	-	-	2.5	4.8
PCL/PVA/PCL	50	18.7	215	80.4	2.5	0.9

Cross-section and schematic representation of the PCL/PVA/PCL scaffold is presented in Figure 1b. PCL solution (10% wt/v) was prepared in glacial acetic acid (Sigma-Aldrich, USA.), which has a freezing temperature around 17°C. To form the bottom layer of the scaffold, 0.7 mL of PCL solution was poured into a 24-well plate and incubated at -80°C overnight. To prepare the PVA layer, 0.5 mL of 10% PVA solution (10% wt/v, dH2O), containing 5 mg/mL of CaFB (Via-Bor, Türkiye) was freeze-dried in a 48-well plate. The PVA sponge was then extracted from the well and placed onto the frozen PCL layer in the 24-well plate. To fill the space surrounding the PVA layer and to achieve the same PCL layer thickness above, 1.4 mL

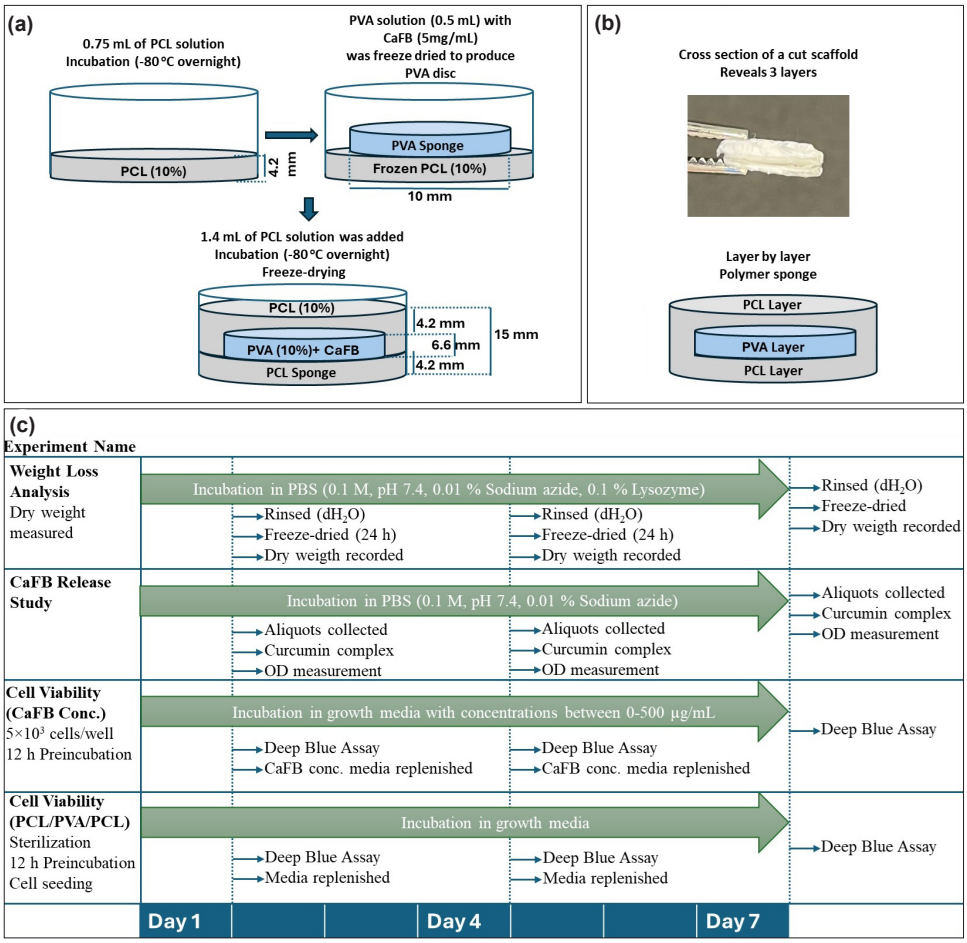

Figure 1. a) Schematic representation of the layer-by-layer scaffold fabrication via freeze drying method. b) Cross section of the PCL/PVA/PCL scaffold and schematic representation of the final form of the layer-by-layer scaffold. c) Diagram showing the experimental steps performed at incubation time points

of PCL solution was added on top of the PVA to form the third layer. The amount of PCL solution needed was calculated according to the volume that will fill the space at the edges of the PVA disc and achieve the same thickness for the top PCL layer. After incubation at -80°C overnight, the plate was freeze-dried to obtain the final layer-by-layer scaffold. The diagram showing the following experiments and incubation time points is presented in Figure 1c.

2.2. Morphological Analysis via Scanning Electron Microscopy

The surface morphology of PCL and PVA layers was characterized via high-resolution field emission scanning electron microscopy (FE-SEM, SU7000, HITACHI, Japan). The surfaces of the samples were coated with a 5 nm gold layer prior to analysis using a vacuum sputter coater (EM ACE 600, Leica, Germany).

2.3. Fourier Transform Infrared (FTIR) Spectroscopy Analysis

Attenuated total reflectance Fourier transform infrared spectroscopy (ATR-FTIR) was used to confirm the chemical structure of CaFB. The IR spectra were recorded using a Spectrum 100 FTIR spectrometer equipped with an ATR accessory (Perkin Elmer, USA). The samples were positioned on the ATR crystal plate and scanned at room temperature across the mid-infrared region (650-4000 cm^{-1}) with a resolution of 4 cm^{-1} in absorbance mode.

2.4. Weight Loss Analysis

After fabricating the layer-by-layer scaffold with freeze-drying, samples were taken out from the wells in which they were cast, and their initial dry weight was measured. To determine the overall hydrolytic and enzymatic degradation rate of the samples over 7 days, they were incubated in a shaking incubator at 37°C (JSR JSSI-300C, Korea), in phosphate buffer solution (PBS) (0.1 M, pH 7.4, 4 mL) containing 0.01 % sodium azide and 0.1 % lysozyme enzyme. A single-layer PVA hydrogel was also tested as the control group for comparison. At each incubation time point, samples were gently rinsed with dH_2O and freeze-dried for 24 h before their weights were recorded. The *in vitro* degradation rate was calculated according to Equ 1.

$$\text{Weight loss } (\%) = \frac{(W_0 - W_t)}{(W_0)} \times 100 \qquad (1)$$

2.5. Study of CaFB Release

To detect CaFB dose-dependent optical density by ultraviolet (UV) absorption, a complex between curcumin and CaFB was formed, and a dose-dependent calibration curve was plotted. Curcumin was initially extracted from turmeric by ethanol extraction method. Briefly, 20 g of turmeric was incubated in an ethanol solution (80%) for 3 h and the solution was filtered through filter paper to remove solid particles from ethanol. Then ethanol was removed under vacuum to obtain the curcumin-bearing extract. Then the weighted extract was resuspended in methanol (10 mg/mL). To study CaFB release, CaFB-loaded PCL/PVA/PCL scaffolds were incubated in 4 mL of PBS (0.1 M, pH 7.4, 0.01 % sodium azide) and aliquots from the release media were collected over 7 days for optical density measurement. For comparison, CaFB release from the single-layer PVA hydrogel was also tested as a control. To detect CaFB in the release media, 1 mL release media and 50 µL of curcumin extract solution were added to an Eppendorf tube and the suspension was vortexed for 1 min. The PBS phase was then removed for optical density measurement at 410 nm wavelength via UV spectrophotometer (PG Instruments Ltd., UK). The amount of CaFB released was calculated from a calibration curve prepared with known concentrations of CaFB.

2.6. In Vitro Cell Viability Analysis

In vitro cell viability tests were conducted using the Saos-2 cell line (ATCC, USA) to determine the effect of different CaFB concentrations on cell metabolism. Dulbecco's Modified Eagle Medium (DMEM) with high glucose, supplemented with 10% fetal bovine serum (FBS) and %1 Penicillin/Streptomycin was used as the growth media. Cell cultures were maintained in a CO_2 incubator (New Brunswick, Galaxy 170 S, Eppendorf, Germany) at 37°C. For the viability experiments to determine concentration-dependent cell viability, 5×10^3 cells/well were seeded in 96-well plate and left for incubation overnight. CaFB was dissolved in the cell media at concentrations ranging between 0-500 µg/mL and introduced to the wells. The Deep Blue cell viability kit (Biolegend, USA) was used to measure cell viability after 1, 4, and 7 days of incubation. Briefly, the Deep Blue solution was added to the wells to achieve a final concentration of 10% (v/v) and the plate was incubated for 4 h at 37°C. Deep Blue solutions were then transferred to a new 96-well plate to measure fluorescence at 535 nm excitation and 590 nm emission with a microplate reader (Varioskan Lux, Thermo Scientific, USA). The media in all the wells were replaced with fresh media, maintaining the same CaFB concentrations and incubation continued. Results were compared to the control group, which did not contain CaFB.

The effect of direct contact with CaFB releasing scaffold on cell viability was analyzed by direct seeding of cells on the surface of the scaffold. After the scaffold was fabricated via freeze-drying, each surface of the samples was sterilized with UV light for 30 min in a well plate. The samples were then incubated in cell media overnight and the wet scaffolds were used for cell seeding after the media was removed. Cells (2.5×10^4 cells/scaffold) were transferred to the scaffold surface in a 20 µL drop of media and incubated for 2 h in a humidified CO_2 incubator to ensure that the cells attached to the scaffold. Each well was then filled with media to cover the scaffolds. Deep Blue tests were conducted on days 1, 4, and 7. Media for each scaffold was changed to fresh DMEM media on the test days.

2.7. Statistical Analysis

Statistically significant differences between experimental groups were calculated using SPSS software (Version 22, IBM, USA). Independent samples t-tests and One-Way Analysis of Variance (ANOVA) were used to compare mean values and measure statistically significant differences between groups. The level of significance was set at $P<0.05$.

3. Results and Discussion

The surface micro-nano morphology of the layered scaffold was observed by FE-SEM analyses and the morphology of the inner PVA layer was observed after separating the scaffold layers (Figure 2).

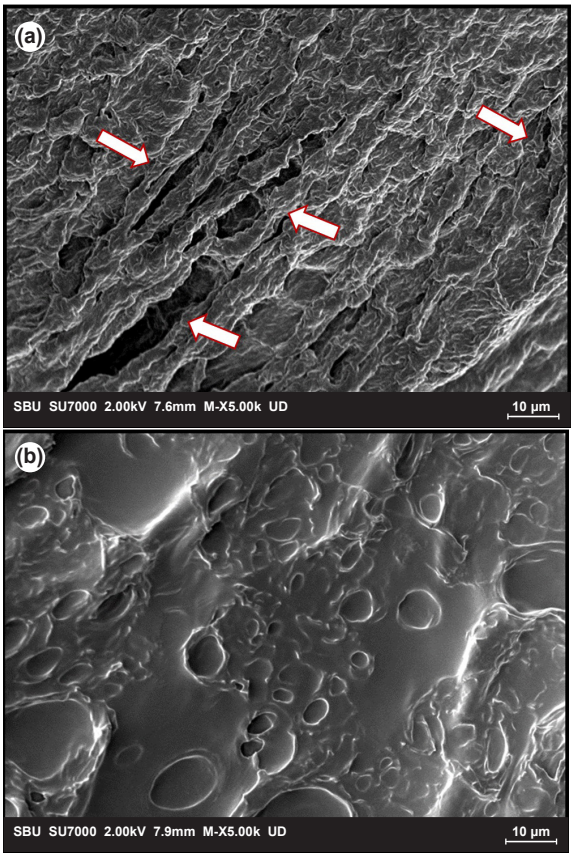

Figure 2. FE-SEM images of scaffold layers, PCL (a) and PVA (b). Arrows show the pores that have been created on the surface. Images were taken at 5000X magnification and scale bars show 10 µm length

PCL layer was designed to surround the surface of the inner PVA layer of the scaffold to control the release of CaFB from the inner PVA layer. FE-SEM images of the PCL layer present a rough surface with pores that connect to the depths of the layer (Figure 2a). Pore size is one of the factors that determines the interaction of bone cells with the scaffold which will determine cell fate and tissue regeneration [31]. Porous structure and interconnectivity in scaffolds have been reported to be essential for osteoconduction. A minimum pore size of 100 µm has been reported to be essential for osteointegration and pores larger than 300 µm have been reported to be needed for the vascularization of the healing bone tissue [32]. Surface with a smaller pore size of around 62 µm has been reported to promote osteogenic gene expression (RUNX2, ALP, BSP, COL, and OPN) while viability and proliferation of osteoblast cells were reported to be improved on surfaces with larger pores [33]. A study of Lee et al. has evaluated the interaction of MG63 osteoblast-like cells with PCL membrane surfaces that have pore sizes between 0.2 to 8 µm. Studies have revealed that as the pore size increases and gets closer to 8 µm, cell differentiation and matrix production are increased which was observed by higher total protein synthesis and ALP specific activity [34]. These results have shown that the effect of porosity on osteoblast-like cells can vary on different surfaces and has no strict boundaries. The outermost surface of the PCL/PVA/PCL scaffold is the PCL layer and SEM images of the PCL surface have revealed micropores between 2 to 10 µm. The observed pore diameter has previously been associated with enhanced cell differentiation, and matrix production in osteoblast-like cells [34]. Also, after implantation, the polymer surface is expected to biodegrade over time, and this biodegradation could open new pores and increase the diameter of the existing pores which will support better osteointegration. The presence of surface roughness is known to enhance osteoblasts attachment and adhesion while improving osteogenic activity and mineralization [35,36]. Therefore, roughness is expected to support a better interaction with bone tissue and create an osteoconductive scaffold. Surface roughness is also known to increase protein adhesion which will improve cell adhesion and differentiation of bone cells was reported to be enhanced on rough surfaces compared to smooth surfaces [37]. On the other hand, the inner layer of the scaffold, the PVA layer, has shown a smoother micro-nano surface topography with close pore structures. The main role of the PVA layer is to carry CaFB in the core of the scaffold and support the controlled release of CaFB over time. Therefore, the PVA layer is not expected to have direct contact with regenerating tissue as PVA polymer will also leave the scaffold over time by degradation.

FTIR analysis was performed to verify the chemical structure of CaFB (Figure 3). The broad band centered at 3247 cm^{-1} was observed in the IR spectrum of metal complexes of saccharides and can be attributed to the

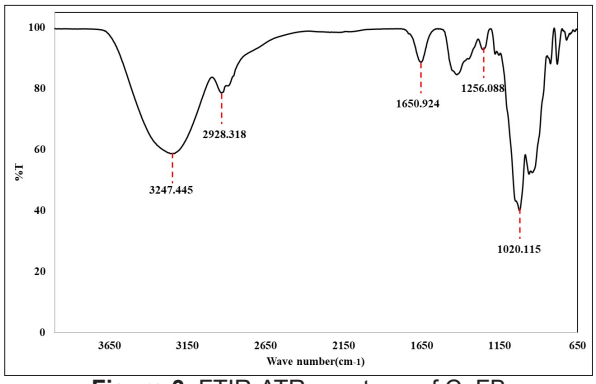

Figure 3. FTIR-ATR spectrum of CaFB

B-O bond. The stretching of the CH_2 group creates a band at 2928 cm^{-1} with a shoulder around 2880 cm^{-1}. The band at 1650 cm^{-1} is attributed to the stretching motion of the terminal B-O linkage of fructoborate [15]. The IR spectrum formed by chemical groups CH, OH, COH, CH_2OH, and CH_2 in the CaFB structure can be observed in the bands around 1421 cm^{-1} and a band created by water crystallization can be seen at 1256 cm^{-1}. Vibrational bands of characteristics groups to fructose and CaFB, CO, CH_2OH, C-CH, CH_2, C-C, and C-O-C, can be observed between 1200 to 650 cm^{-1} [38].

Weight loss analysis of the scaffold was conducted in PBS solution that contains lysozyme enzyme (Figure 4a). Lysozyme was added to mimic physiologic conditions since lysozyme is a common enzyme that exists in blood and serum. The use of the enzyme also mimics the wound site since the natural level

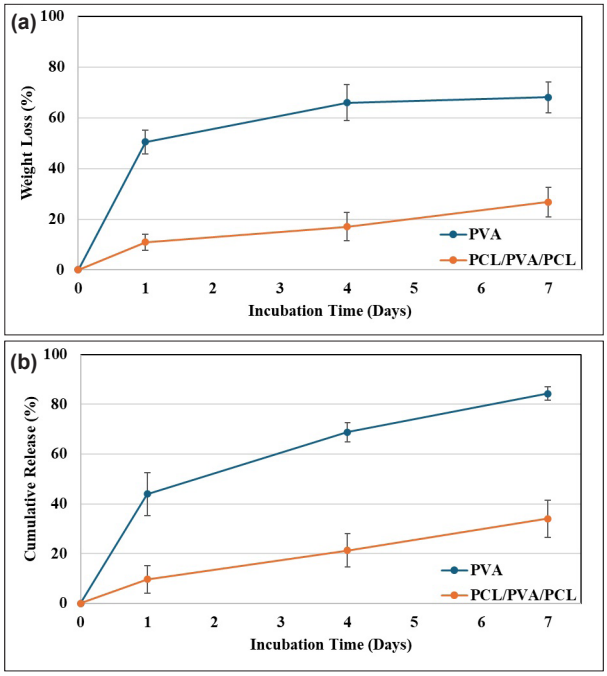

Figure 4. Percent weight loss of single-layered PVA hydrogel and PCL/PVA/PCL scaffold through 7 days of incubation in PBS supplemented with lysozyme (a) and percent CaFB cumulative release of single-layered PVA hydrogel and PCL/PVA/PCL scaffold through 7 days of incubation in PBS (b)

of this enzyme increases in tissues when there is an inflammation or infection [39]. PCL is a hydrophobic biodegradable polymer that has long-term stability in the body and is expected to remain structurally stable *in vitro* with little to no degradation in several weeks [40]. The tri-layered scaffold was produced by freeze-drying and during the freezing step, PVA polymer chains form intermolecular and intramolecular hydrogen bonds and crystalline regions which achieve physical crosslinking [41]. Although PVA is a water-soluble polymer, the ability of PVA to form physical crosslinking has previously been reported to decrease its degradation rate and weight loss in aqueous environment. Previous studies have applied several freeze and thaw cycles to improve physical crosslinking and achieved slower degradation [42-44]. On the other hand, in this study PVA layer was produced via freeze dryer, directly after freezing in order to avoid further delaying PVA degradation, thereby promoting CaFB release. Also, a hydrophobic PCL layer was fabricated to cover the PVA surface to control CaFB release. When PVA as a single layer was incubated for 24 h, 50.41±4.7% of the hydrogel was lost. After 3 and 7 days in PBS, weight loss of the single-layer PVA scaffold has increased to 65.9±7.1% and 68.03±6.1% (Figure 4a). The initial fast degradation can be attributed to polymer chains that did not form entanglement and physical crosslinking. After initial mass loss, the weight of the hydrogel remained stable. Weight loss of the tri-layered scaffold was lower compared to the single-layer PVA scaffold (26.8±5.7% at 7 days of incubation). Also, initial weight loss was only at 10.8±3.1% after one day of incubation. This is due to the hydrophobic PCL layer covering the PVA surface and slowing down the water diffusion into the PVA layer [45]. Since the PCL layer covering the PVA will decrease the diffusion of aqueous media, the weight loss of the PVA layer will be lower in the same incubation period. The same reason also created a control mechanism for CaFB release from the scaffold groups and achieved long-term release (Figure 4b). The single-layer PVA hydrogel created a burst CaFB release of 43.9±8.6% on day one and achieved a cumulative release of 84.2±2.6% after 7 days of release. On the other hand, the PCL layer surrounding the tri-layered scaffold was able to control and prevent the bust release of CaFB achieving a steady increase in cumulative release with a 33.9±7.4% release after 7 days. Tri-layered design of the scaffold has proven to be successful in controlling the release of CaFB.

The effect of CaFB dose on Saos-2 cell viability was analyzed with CaFB concentrations between 1.95 to 500 µg/ml after 1, 4, and 7 days of incubation (Figure 5a). Results have shown that, even at concentrations as high as 500 µg/ml, CaFB has not shown a negative effect on cells, and viability was preserved through 7 days. After 1 and 4 days of incubation cells treated with 31.25 µg/ml CaFB have shown improved cell viability. After 7 days of incubation, cell viability was higher in groups treated with 250, 125, 62.5, and 31.25 µg/ml CaFB concentrations. In the second trial for cell viability, Saos-2 cells were directly seeded onto the PCL/PVA/PCL scaffold with CaFB loaded inside the PVA layer at the core (Figure 5b). The results of cell viability under different CaFB doses and CaFB release studies were considered to decide the amount of CaFB that will be loaded into the PCL/PVA/PCL scaffold. The CaFB dose study has shown that CaFB concentration between 62.5 and 250 µg/mL has supported the highest cell viability after 7 days of incubation. According to the results of the release study, after 1, 4, and 7 days of incubation, the cumulative release of CaFB was expected to be roughly around 9.7, 21.2, and 33.9%. With an initial CaFB loading of 2.5 mg, the scaffold was expected to release, 60.6, 71.9, and 79.3 µg/mL CaFB between incubation time points in 4 mL of media when media replenishment was also considered. To obtain a steady CaFB release within the effective dose, 2.5 mg of CaFB was loaded into the scaffold. Results showed that the PCL/PVA/PCL scaffold has supported the viability of cells through 7 days when compared to a monolayer of cells seeded in a well. After 7 days of incubation, the viability of cells on the scaffold was slightly higher as compared to the control group. The CaFB release from the tri-layered scaffold was shown to be at a slow rate and reaching 33.9±7.4% after 7 days and the CaFB dose study revealed that CaFB treatment starts to improve cell viability after 7 days of incubation at certain concentrations. This could explain why the CaFB-releasing scaffold improved

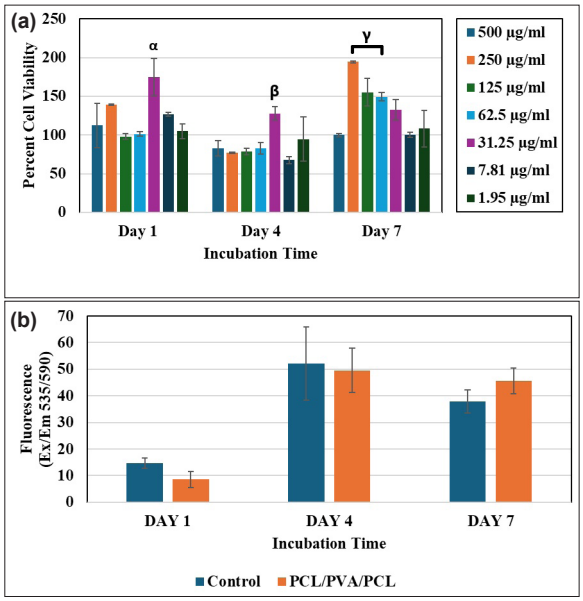

Figure 5. The effect of CaFB concentrations on Saos-2 cell viability through 7 days of incubation. The percent cell viability was calculated with respect to cells incubated with only growth media without CaFB as the control (a). Saos-2 cell viability through 7 days of incubation on control well and PCL/PVA/PCL scaffold (b). α: Statistically significant difference of 31.25 µg/ml group from other groups at day 1 of incubation ($P<0.05$). β: Statistically significant difference of 31.25 µg/ml group from other groups except group 1.95 µg/ml at day 4 ($P<0.05$). γ: Statistically significant difference of 250, 125 and 62.5 µg/ml groups from 500, 7.81, 1.95 µg/ml groups at day 7 ($P<0.05$)

viability after 7 days when compared to the control. The calcium and boron ions in CaFB were responsible for enhanced viability of Saos-2 cells which are known to promote osteogenic activities and enhance bone cell viability [46,47]. The study of Capati et al. analyzed the effects of boron on osteoblastic activity in NOS-1 cells i*n vitro* and reported that even in low concentrations, boron promotes proliferation and differentiation [10]. Another study showed that boron is able to improve bone health and strength *in vivo* in rabbits [4]. CaFB was previously reported to increase osteopontin and osteocalcin expression in bone tissue and the boron that it contains has a role in increasing the expression of genes responsible for mineralization and hormones like 17β-estradiol (E2) and testosterone) [12,48]. A pilot study that treats 13 middle-aged subjects who are deficient in vitamin D with CaFB supplementation for 60 days, has reported a significant increase in 25 (OH) vitamin D levels [3]. This shows that CaFB can also improve bone health by regulating Vitamin D metabolism. Several previous studies have also adapted PCL/PVA/PCL layered scaffold structure and used different fabrication techniques to achieve this layered formation. Study of Harmanci et al. used 3D printing to achieve PCL/PVA/PCL layered scaffold for diabetic wound healing and evaluated scaffolds' biocompatibility by testing viability of human fibroblast cell line (HFF-1) *in vitro*. HFF-1 cell viability on PCL/PVA/PCL scaffold was reported to be biocompatible with around 89.2% viability after 7 days [26]. Another study has also produced a PCL/PVA/PCL layered scaffold by electrospinning to assess the wound-healing potential of the scaffold. Biocompatibility of the scaffold was evaluated on the L929 mouse fibroblast cell line and the PCL/PVA/PCL scaffold was found to be compatible with over 80% viability after 2 days [27]. PCL and PVA polymers have also been used in bone tissue engineering studies in fiber forms which were produced by layers or blends [49-53]. Previously, co-axial fibers have been fabricated by PCL shell and PVA core, and fabricated scaffold has shown to support the viability and osteogenic differentiation of mesenchymal stem cells [49]. Pattanashetti et al., demonstrated biocompatibility of multilayered PCL/PVA scaffolds by showing the proliferation of MG-63 bone osteosarcoma cells [53]. Ebrahimi et al. reported the biocompatibility of PCL/PVA nanofibrous membranes and showed that membranes support the differentiation of human endometrial stem cells to osteogenic linage [51]. Similarly, Maheshwari et al. reported enhanced adhesion and proliferation of MG-63 osteoblast cells on PVA/HAp/PCL scaffolds [52]. These studies have shown the potential of PCL/PVA composite scaffold used for bone tissue engineering. This study demonstrated the fabrication of a PCL/PVA/PCL scaffold via freeze-drying method and proved that the PCL/PVA/PCL scaffold supports the viability of Saos-2 cells.

The results of this study have shown that local release of CaFB from a bone scaffold can improve bone tissue regeneration by controlled release of CaFB. The results showed that a designed layered scaffold was able to control the release of CaFB and loading of CaFB into a biodegradable scaffold was found to be a promising approach for local delivery. Additionally, CaFB has shown to increase cell viability while CaFB-loaded scaffold was successfully supported cell viability. These results have supported the hypothesis of the study by proving control of the PCL/PVA/PCL scaffold on CaFB release and the ability of the scaffold to support cell viability.

4. Conclusions

This study has demonstrated the production of a CaFB-releasing polymeric scaffold system for bone tissue regeneration. A tri-layered PCL/PVA/PCL scaffold was designed to carry CaFB within the hydrophilic PVA core and the core was surrounded by hydrophobic PCL polymer. The presence of the PCL layer has been shown to successfully control PVA weight loss, achieving a stable scaffold structure. The hydrophobic PCL layer was also successful in slowing down the CaFB release rate by limiting the rate of water diffusion. An *in vitro* study has shown that CaFB has dose dependent effect on Saos-2 cell viability and the highest improvement in viability was recorded after 7 days of CaFB treatment. The fabricated CaFB-releasing tri-layered PCL/PVA/PCL scaffold has supported cell viability through 7 days and was shown to be biocompatible. This study has shown that controlled release of CaFB can be achieved with polymeric scaffolds and scaffolds carrying CaFB are promising as biomaterials to improve bone tissue regeneration.

5. Acknowledgements

CaFB was a kind gift from Via-Bor (Türkiye). The FTIR-ATR analysis was performed by Yıldız Technical University, Application and Research Center for Science and Technology (BİTUAM).

References

[1] Rondanelli, M., Faliva, M. A., Peroni, G., Infantino, V., Gasparri, C., Iannello, G., … & Tartara, A. (2020). Pivotal role of boron supplementation on bone health: A narrative review. *Journal of Trace Elements in Medicine and Biology*, *62*, 126577. https://doi.org/10.1016/J.JTEMB.2020.126577

[2] Mahdavi, R., Belgheisi, G., Haghbin-Nazarpak, M., Omidi, M., Khojasteh, A., & Solati-Hashjin, M. (2020). Bone tissue engineering gelatin-hydroxyapatite/graphene oxide scaffolds with the ability to release vitamin D: fabrication, characterization, and in vitro study. *Journal of Materials Science: Materials in Medicine*, *31*(11), 97. https://doi.org/10.1007/s10856-020-06430-5

[3] Miljkovic, D., Miljkovic, N., & McCarty, M. F. (2004). Up-regulatory impact of boron on vitamin D function-Does it reflect inhibition of 24-hydroxylase? *Medical Hypotheses*, *63*(6), 1054-1056. https://doi.org/10.1016/j.mehy.2003.12.053

[4] Hakki, S. S., Dundar, N., Kayis, S. A., Hakki, E. E., Hamurcu, M., Kerimoglu, U., … & Nielsen, F. H. (2013). Boron enhances strength and alters mineral composition of bone in rabbits fed a high energy diet. *Journal of Trace Elements in Medicine and Biology*, *27*(2), 148-153. https://doi.org/10.1016/J.JTEMB.2012.07.001

[5] Armstrong, T. A., Spears, J. W., Crenshaw, T. D., & Nielsen, F. H. (2000). Boron supplementation of a semipurified diet for weanling pigs improves feed efficiency and bone strength characteristics and alters plasma lipid metabolites. *The Journal of Nutrition*, *130*(10), 2575-2581. https://doi.org/10.1093/jn/130.10.2575

[6] Naghii, M. R., Torkaman, G., & Mofid, M. (2006). Effects of boron and calcium supplementation on mechanical properties of bone in rats. *BioFactors*, *28*(3-4), 195-201. https://doi.org/10.1002/biof.5520280306

[7] Nielsen, F. H., & Stoecker, B. J. (2009). Boron and fish oil have different beneficial effects on strength and trabecular microarchitecture of bone. *Journal of Trace Elements in Medicine and Biology*, *23*(3), 195-203. https://doi.org/10.1016/j.jtemb.2009.03.003

[8] Ying, X., Cheng, S., Wang, W., Lin, Z., Chen, Q., Zhang, W., … & Lu, C. Z. (2011). Effect of boron on osteogenic differentiation of human bone marrow stromal cells. *Biological Trace Element Research*, *144*(1-3), 306-315. https://doi.org/10.1007/s12011-011-9094-x

[9] Hakki, S. S., Bozkurt, B. S., & Hakki, E. E. (2010). Boron regulates mineralized tissue-associated proteins in osteoblasts (MC3T3-E1). *Journal of Trace Elements in Medicine and Biology*, *24*(4), 243-250. https://doi.org/10.1016/j.jtemb.2010.03.003

[10] Capati, M. L. F., Nakazono, A., Igawa, K., Ookubo, K., Yamamoto, Y., Yanagiguchi, K., … & Hayashi, Y. (2016). Boron accelerates cultured osteoblastic cell activity through calcium flux. *Biological Trace Element Research*, *174*(2), 300-308. https://doi.org/10.1007/s12011-016-0719-y

[11] Seydibeyoğlu, M. Ö., Caka, M., Ulucan-Karnak, F., Onak, G., Uzel, A., Ozyildiz, F., & Karaman, O. (2021). Bone cement formulation with reduced heating of bone cement resin. *Journal of Boron*, *6*(2), 274-282. https://doi.org/10.30728/BORON.835919

[12] Uysal, İ., Yılmaz, B., & Evis, Z. (2020). Boron doped hydroxapatites in biomedical applications. *Journal of Boron*, *5*(4), 199-208. https://doi.org/10.30728/BORON.734804

[13] Aki, D., Ulag, S., Unal, S., Sengor, M., Ekren, N., Lin, C. C., … & Gunduz, O. (2020). 3D printing of PVA/hexagonal boron nitride/bacterial cellulose composite scaffolds for bone tissue engineering. *Materials & Design*, *196*, 109094. https://doi.org/10.1016/J.MATDES.2020.109094

[14] Butan, S., Filimon, V., & Bounegru, A. V. (2024). Human health impact and advanced chemical analysis of fructoborates: A comprehensive review. *Chemical Papers*, *78*(9), 5151-5167. https://doi.org/10.1007/S11696-024-03428-Z/FIGURES/6

[15] Wagner, C. C., Ferraresi Curotto, V., Pis Diez, R., & Baran, E. J. (2008). Experimental and theoretical studies of calcium fructoborate. *Biological Trace Element Research*, *122*(1), 64-72. https://doi.org/10.1007/s12011-007-8060-0

[16] Capozzi, A., Scambia, G., & Lello, S. (2020). Calcium, vitamin D, vitamin K2, and magnesium supplementation and skeletal health. *Maturitas*, *140*, 55-63. https://doi.org/10.1016/J.MATURITAS.2020.05.020

[17] Marie, P. J. (2010). The calcium-sensing receptor in bone cells: A potential therapeutic target in osteoporosis. *Bone*, *46*(3), 571-576. https://doi.org/10.1016/j.bone.2009.07.082

[18] Chai, Y. C., Carlier, A., Bolander, J., Roberts, S. J., Geris, L., Schrooten, J., … & Luyten, F. P. (2012). Current views on calcium phosphate osteogenicity and the translation into effective bone regeneration strategies. *Acta Biomaterialia*, *8*(11), 3876-3887. https://doi.org/10.1016/j.actbio.2012.07.002

[19] Mogoşanu, G. D., Biţă, A., Bejenaru, L. E., Bejenaru, C., Croitoru, O., Rău, G., … & Scorei, R. I. (2016). Calcium fructoborate for bone and cardiovascular health. *Biological Trace Element Research*, *172*(2), 277-281. https://doi.org/10.1007/s12011-015-0590-2

[20] Turck, D., Castenmiller, J., De Henauw, S., Hirsch-Ernst, K. I., Kearney, J., Maciuk, A., … & Knutsen, H. K. (2021). Safety of calcium fructoborate as a novel food pursuant to Regulation (EU) 2015/2283. *EFSA Journal*, *19*(7). https://doi.org/10.2903/j.efsa.2021.6661

[21] Manda, D., Popa, O., Vladoiu, S., & Dumitrache, C. (2009). Calcium fructoborate effect on osteoblast mineralization in vitro. *Bone*, *44*, S298-S299. https://doi.org/10.1016/J.BONE.2009.03.545

[22] Scorei, R. I., & Rotaru, P. (2011). Calcium fructoborate-Potential anti-inflammatory agent. *Biological Trace Element Research*, *143*(3), 1223-1238. https://doi.org/10.1007/s12011-011-8972-6

[23] Văruţ, R. M., Melinte, P. R., Pîrvu, A. S., Gîngu, O., Sima, G., Oancea, C. N., … & Neamţu, J. (2020). Calcium fructoborate coating of titanium-hydroxyapatite implants by chemisorption deposition improves implant osseointegration in the femur of New Zealand White rabbit experimental model. *Romanian Journal of Morphology and Embryology*, *61*(4), 1235-1247. https://doi.org/10.47162/RJME.61.4.25

[24] Scorei, I. D., & Scorei, R. I. (2013). Calcium fructoborate helps control inflammation associated with diminished bone health. *Biological Trace Element Research*, *155*(3), 315-321. https://doi.org/10.1007/s12011-013-9800-y

[25] Marone, P. A., Heimbach, J. T., Nemzer, B., & Hunter, J. M. (2016). Subchronic and genetic safety evaluation of a calcium fructoborate in rats. *Food and Chemical Toxicology*, *95*, 75-88. https://doi.org/10.1016/j.fct.2016.06.021

[26] Harmanci, S., Dutta, A., Cesur, S., Sahin, A., Gunduz, O., Kalaskar, D. M., & Ustundag, C. B. (2022). Production of 3D printed bi-layer and tri-layer sandwich scaffolds with polycaprolactone and poly (vinyl alcohol)-metformin towards diabetic wound healing. *Polymers*, *14*(23), 5306. https://doi.org/10.3390/polym14235306

[27] Saeed, S. M., Mirzadeh, H., Zandi, M., & Barzin, J. (2017). Designing and fabrication of curcumin loaded

PCL/PVA multi-layer nanofibrous electrospun structures as active wound dressing. *Progress in Biomaterials*, *6*(1-2), 39-48. https://doi.org/10.1007/s40204-017-0062-1

[28] Ghiyasi, Y., Salahi, E., & Esfahani, H. (2021). Synergy effect of Urtica dioica and ZnO NPs on microstructure, antibacterial activity and cytotoxicity of electrospun PCL scaffold for wound dressing application. *Materials Today Communications*, *26*, 102163. https://doi.org/10.1016/j.mtcomm.2021.102163

[29] Govender, M., Indermun, S., Kumar, P., Choonara, Y. E., & Pillay, V. (2018). 3D printed, PVA-PAA hydrogel loaded-polycaprolactone scaffold for the delivery of hydrophilic in-situ formed sodium indomethacin. *Materials*, *11*(6), 1006. https://doi.org/10.3390/ma11061006

[30] Dvorakova, J., Wiesnerova, L., Chocholata, P., Kulda, V., Landsmann, L., Cedikova, M., … & Babuska, V. (2023). Human cells with osteogenic potential in bone tissue research. *BioMedical Engineering OnLine*, *22*(1), 33. https://doi.org/10.1186/s12938-023-01096-w

[31] Arpornmaeklong, P., Suwatwirote, N., Pripatnanont, P., & Oungbho, K. (2007). Growth and differentiation of mouse osteoblasts on chitosan-collagen sponges. *International Journal of Oral and Maxillofacial Surgery*, *36*(4), 328-337. https://doi.org/10.1016/j.ijom.2006.09.023

[32] Ratnayake, J. T. B., Gould, M. L., Shavandi, A., Mucalo, M., & Dias, G. J. (2017). Development and characterization of a xenograft material from New Zealand sourced bovine cancellous bone. *Journal of Biomedical Materials Research Part B: Applied Biomaterials*, *105*(5), 1054-1062. https://doi.org/10.1002/jbm.b.33644

[33] Teixeira, L. N., Crippa, G. E., Lefebvre, L.-P., De Oliveira, P. T., Rosa, A. L., & Beloti, M. M. (2012). The influence of pore size on osteoblast phenotype expression in cultures grown on porous titanium. *International Journal of Oral and Maxillofacial Surgery*, *41*(9), 1097-1101. https://doi.org/10.1016/j.ijom.2012.02.020

[34] Lee, S. J., Choi, J. S., Park, K. S., Khang, G., Lee, Y. M., & Lee, H. B. (2004). Response of MG63 osteoblast-like cells onto polycarbonate membrane surfaces with different micropore sizes. *Biomaterials*, *25*(19), 4699-4707. https://doi.org/10.1016/j.biomaterials.2003.11.034

[35] Dwivedi, R., Kumar, S., Pandey, R., Mahajan, A., Nandana, D., Katti, D. S., & Mehrotra, D. (2020). Polycaprolactone as biomaterial for bone scaffolds: Review of literature. *Journal of Oral Biology and Craniofacial Research*, *10*(1), 381-388. https://doi.org/10.1016/j.jobcr.2019.10.003

[36] Filipov, E., Angelova, L., Vig, S., Fernandes, M. H., Moreau, G., Lasgorceix, M., … & Daskalova, A. (2022). Investigating potential effects of ultra-short laser-textured porous poly-ε-caprolactone scaffolds on bacterial adhesion and bone cell metabolism. *Polymers*, *14*(12), 2382. https://doi.org/10.3390/polym14122382

[37] Melčová, V., Krobot, Š., Šindelář, J., Šebová, E., Rampichová, M. K., & Přikryl, R. (2024). The effect of surface roughness and wettability on the adhesion and proliferation of Saos-2 cells seeded on 3D printed poly(3-hydroxybutyrate)/polylactide (PHB/PLA) surfaces. *Results in Surfaces and Interfaces*, *16*, 100271. https://doi.org/10.1016/j.rsurfi.2024.100271

[38] Rotaru, P., Scorei, R., Hărăbor, A., & Dumitru, M. D. (2010). Thermal analysis of a calcium fructoborate sample. *Thermochimica Acta*, *506*(1-2), 8-13. https://doi.org/10.1016/j.tca.2010.04.006

[39] Lan, W., Zhang, X., Xu, M., Zhao, L., Huang, D., Wei, X., & Chen, W. (2019). Carbon nanotube reinforced polyvinyl alcohol/biphasic calcium phosphate scaffold for bone tissue engineering. *RSC Advances*, *9*(67), 38998-39010. https://doi.org/10.1039/C9RA08569F

[40] Yoshioka, T., Kamada, F., Kawazoe, N., Tateishi, T., & Chen, G. (2010). Structural changes and biodegradation of PLLA, PCL, and PLGA sponges during in vitro incubation. *Polymer Engineering & Science*, *50*(10), 1895-1903. https://doi.org/10.1002/pen.21714

[41] Waresindo, W. X., Luthfianti, H. R., Edikresnha, D., Suciati, T., Noor, F. A., & Khairurrijal, K. (2021). A freeze-thaw PVA hydrogel loaded with guava leaf extract: physical and antibacterial properties. *RSC Advances*, *11*(48), 30156-30171. https://doi.org/10.1039/D1RA04092H

[42] Wu, F., Gao, J., Xiang, Y., & Yang, J. (2023). Enhanced mechanical properties of PVA hydrogel by low-temperature segment self-assembly vs. freeze-thaw cycles. *Polymers*, *15*(18), 3782. https://doi.org/10.3390/polym15183782

[43] Lotfipour, F., Alami-Milani, M., Salatin, S., Hadavi, A., & Jelvehgari, M. (2019). Freeze-thaw-induced cross-linked PVA/chitosan for oxytetracycline-loaded wound dressing: The experimental design and optimization. *Research in Pharmaceutical Sciences*, *14*(2), 175. https://doi.org/10.4103/1735-5362.253365

[44] Adelnia, H., Ensandoost, R., Shebbrin Moonshi, S., Gavgani, J. N., Vasafi, E. I., & Ta, H. T. (2022). Freeze/thawed polyvinyl alcohol hydrogels: Present, past and future. *European Polymer Journal*, *164*, 110974. https://doi.org/10.1016/j.eurpolymj.2021.110974

[45] Zhou, X., Hou, C., Chang, T.-L., Zhang, Q., & Liang, J. F. (2020). Controlled released of drug from doubled-walled PVA hydrogel/PCL microspheres prepared by single needle electrospraying method. *Colloids and Surfaces B: Biointerfaces*, *187*, 110645. https://doi.org/10.1016/j.colsurfb.2019.110645

[46] Della Pepa, G. (2016). Microelements for bone boost: the last but not the least. *Clinical Cases in Mineral and Bone Metabolism*. https://doi.org/10.11138/ccmbm/2016.13.3.181

[47] Decker, S., Arango-Ospina, M., Rehder, F., Moghaddam, A., Simon, R., Merle, C., … & Westhauser, F. (2022). In vitro and in ovo impact of the ionic dissolution products of boron-doped bioactive silicate glasses on cell viability, osteogenesis and angiogenesis. *Scientific Reports*, *12*(1), 8510. https://doi.org/10.1038/s41598-022-12430-y

[48] Uzunçakmak, S. K. (2023). Sıçanlarda borik asit, kalsiyum fruktoborat ve potasyum bor sitratın kemik sağlığı ve sistemik inflamatuvar belirteçler üzerine etkisi. *Bor Dergisi*, *8*(1), 9-15. https://doi.org/10.30728/BORON.1142574

[49] Prosecká, E., Buzgo, M., Rampichová, M., Kocourek, T., Kochová, P., Vysloužilová, L., … & Amler, E. (2012).

Thin-layer hydroxyapatite deposition on a nanofiber surface stimulates mesenchymal stem cell proliferation and their differentiation into osteoblasts. *Journal of Biomedicine and Biotechnology*, 2012, 1-10. https://doi.org/10.1155/2012/428503

[50] Mahalingam, S., Bayram, C., Gultekinoglu, M., Ulubayram, K., Homer-Vanniasinkam, S., & Edirisinghe, M. (2021). Co-axial gyro-spinning of PCL/PVA/ha core-sheath fibrous scaffolds for bone tissue engineering. *Macromolecular Bioscience*, *21*(10). https://doi.org/10.1002/mabi.202100177

[51] Ebrahimi, L., Farzin, A., Ghasemi, Y., Alizadeh, A., Goodarzi, A., Basiri, A., … & Ai, J. (2021). Metformin-loaded PCL/PVA fibrous scaffold preseeded with human endometrial stem cells for effective guided bone regeneration membranes. *ACS Biomaterials Science & Engineering*, *7*(1), 222-231. https://doi.org/10.1021/acsbiomaterials.0c00958

[52] Uma Maheshwari, S., Samuel, V. K., & Nagiah, N. (2014). Fabrication and evaluation of (PVA/HAp/PCL) bilayer composites as potential scaffolds for bone tissue regeneration application. *Ceramics International*, *40*(6), 8469-8477. https://doi.org/10.1016/j.ceramint.2014.01.058

[53] Pattanashetti, N. A., Achari, D. D., Torvi, A. I., Doddamani, R. V., & Kariduraganavar, M. Y. (2020). Development of multilayered nanofibrous scaffolds with PCL and PVA:NaAlg using electrospinning technique for bone tissue regeneration. *Materialia*, *12*, 100826. https://doi.org/10.1016/j.mtla.2020.100826